

# Comparison of gas phase and condensed phase $S_Ni$ reactions. The competitive four- and five-centre cyclisations of the 3,4-epoxybutoxide anion. A joint experimental and theoretical study

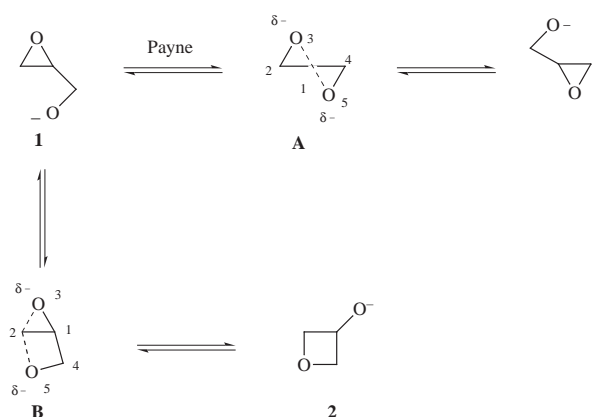
John M. Hevko, Suresh Dua, Mark S. Taylor and John H. Bowie

Department of Chemistry, The University of Adelaide, South Australia, 5005

*Ab initio* calculations [at the MP2-Fc/6-31+G(d) level] indicate that the 3,4-epoxybutoxide anion should undergo competitive  $S_Ni$  cyclisations (through four- and five-membered transition states) to yield the (M – H)<sup>–</sup> ions of oxetan-2-ylmethanol and tetrahydrofuran-3-ol respectively. The barriers to the transition states are comparable (*ca.* 70 kJ mol<sup>–1</sup>) for each process, and the latter product is the more stable by 82 kJ mol<sup>–1</sup> at the level of theory indicated. Gas phase studies of the 3,4-epoxybutoxide anion excited by collisional activation are in accord with this scenario, and show, in addition, that deprotonated 2-oxetanylmethanol can convert to the starting material. Base treatment of 2-(oxiran-2-yl)ethan-1-ol (3,4-epoxybutan-1-ol) in two different solvent systems [10% aqueous sodium hydroxide and sodium hydride–tetrahydrofuran (both at reflux)] yields the same two products observed in the gas phase studies. However, deprotonated tetrahydrofuran-3-ol is the kinetic product in both solvent systems.

## Introduction

The energised 2,3-epoxypropoxide anion undergoes two competing  $S_Ni$  processes in the gas phase: these are summarised in Scheme 1. The more facile of the two processes is the Payne



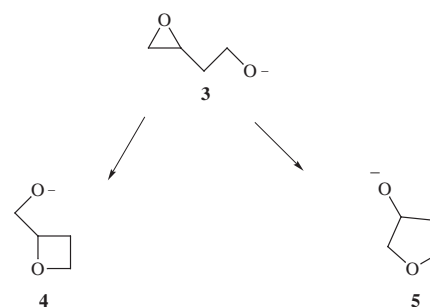
**Scheme 1** A: C<sup>1</sup>O<sup>3</sup> = 1.89, C<sup>1</sup>O<sup>5</sup> = 1.89 Å; O<sup>3</sup>C<sup>1</sup>O<sup>5</sup> = 160.15°, O<sup>5</sup>C<sup>1</sup>C<sup>2</sup>O<sup>3</sup> = –159.7°. B: C<sup>2</sup>O<sup>3</sup> = 1.91, C<sup>2</sup>O<sup>5</sup> = 2.08 Å; O<sup>3</sup>C<sup>2</sup>O<sup>5</sup> = 116.5°, O<sup>5</sup>C<sup>2</sup>C<sup>1</sup>O<sup>3</sup> = –153.0°

rearrangement which has a computed barrier (*ab initio* calculations at the G2 level) of only 45 kJ mol<sup>–1</sup>. This process competes with the alternative cyclisation to yield the four-membered oxetane system **2** (barrier 122 kJ mol<sup>–1</sup>).<sup>1</sup>

The angle of approach of O<sup>–</sup> to the receptor carbon in the transition state is the major feature influencing the relative barriers to the transition states **A** and **B** (the OCO angles in the transition states are computed to be 161.5° for the three-centred Payne process, and 116.5° for the four-centred formation of **2**).<sup>1</sup> The closer the OCO angle is to 180° (*i.e.* the closer the geometry is to that of an ideal  $S_N2$  type transition state), the lower the barrier of the  $S_Ni$  process. The strain energies of the various rings have only a minor influence on the competition between the three- and four-centre cyclisations, since the strain energies of ethylene oxide and oxetane are comparable, *i.e.* 112.5 and 107.5 kJ mol<sup>–1</sup> respectively.<sup>2</sup>

In this paper we extend the above study to probe the scenario summarised in Scheme 2. We wish to investigate the  $S_Ni$

reactions of the 3,4-epoxybutoxide anion **3** both theoretically, and experimentally in the gas and condensed phases, in order to answer the following questions. Firstly, do the two  $S_Ni$  processes shown in Scheme 2 occur? Secondly, if both cyclisations do



**Scheme 2**

occur, then (i) is the angle of approach of O<sup>–</sup> to each of the two possible electrophilic carbon centres a major factor controlling competition between the two processes, (ii) is the difference in strain energy (112.5, 107.5 and 25 kJ mol<sup>–1</sup> for ethylene oxide, oxetane and tetrahydrofuran respectively<sup>2</sup>) a significant factor in controlling the relative extents of the two processes, and (iii) do equilibria between **3**, **4** and **5** occur during the experimental conditions, or are the processes **3** to **4** and **3** to **5** irreversible?

## Results and discussion

### 1. The results of *ab initio* calculations

The results of an *ab initio* computational study using GAUSSIAN94<sup>3</sup> for the reactions shown in Scheme 2 are summarised in Fig. 1. The geometries of the local minima and the transition states were optimised at the RHF/6-31+G(d) level of theory. Energies were then refined at the MP2-Fc/6-31+G(d) level. Geometries and energies of **3**, **4** and **5** and the two transition states **C** and **D** are listed in Table 1.

The details shown in Fig. 1 and Table 1 indicate that the barriers to the two transition states are of the same order. The OCO angles in the transition state are 163.4° for the four- (**C**) and 140.3° for the five-centre (**D**) rearrangements respectively, with the dihedral angles being 172.3 and 163.4° respectively.

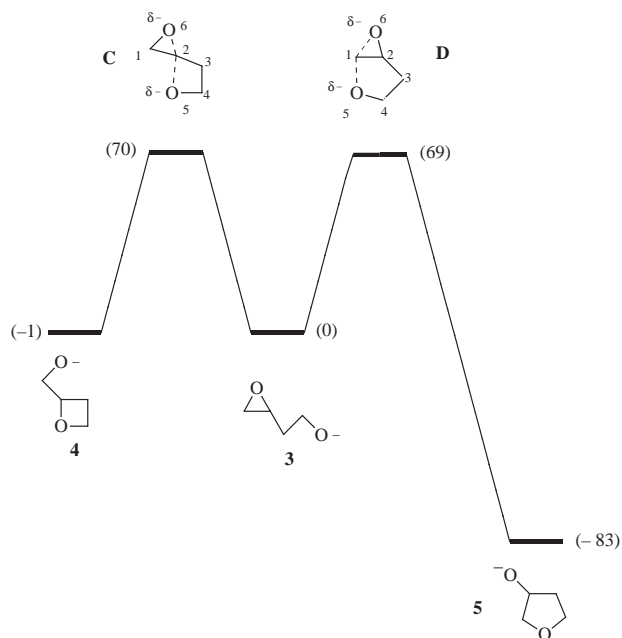


**Fig. 1** *Ab initio* calculations [GAUSSIAN94, geometries RHF/6-31+G(d), energies MP2-Fc/6-31+G(d)] for the competitive  $S_Ni$  cyclisations of the 3,4-epoxybutoxide anion. Partial geometries: **C**,  $C^2O^5 = 2.00$ ,  $C^2O^6 = 1.85$  Å;  $O^6C^2O^5 = 163.4^\circ$ ,  $O^5C^2C^1O^6 = +172.5^\circ$ . **D**,  $C^1O^5 = 2.09$ ,  $C^1O^6 = 1.84$  Å;  $O^6C^1O^5 = 140.3^\circ$ ,  $O^5C^1C^2O^6 = -163.1^\circ$ . For energies and further data on **C** and **D** see Table 1. For other geometries see Supplementary material.

The four-centre  $S_Ni$  reaction has the larger OCO angles in the transition state: these data taken alone favour the kinetic formation of **4**. The change in ring strain from reactant to transition state is another major factor influencing the rate of reaction. The decrease in ring strain from **3** to **C** and **3** to **D** due to the breaking C–O bond should be comparable (C–O = 1.45 Å for **3**, 1.85 Å for **C** and 1.84 Å for **D**). In contrast, the increase in ring strain as a consequence of the formation of the new C–O bond will be greater for **C** [forming C–O bond length = 2.00 Å, strain energy = 107.5 kJ mol<sup>-1</sup> for oxetane<sup>2</sup> (C–O = 1.45 Å)] than for **D** [forming C–O bond length = 2.09 Å, strain energy = 25 kJ mol<sup>-1</sup> for tetrahydrofuran<sup>2</sup> (C–O = 1.45 Å)].

There are two major features which control the rate of a gas phase reaction, *viz.* (i) the barrier to the transition state (described above) and (ii), the frequency or probability factor [of the quasi-equilibrium equation (or the *A* factor of the Arrhenius rate equation)]. The parameters controlling the frequency factor can be complex and an understanding of these depends upon an intimate knowledge of the full potential surface for the reaction (which we do not have). In the simplest scenario, the frequency factors could be a function of the relative probabilities of **3** being able to enter the two competing  $S_Ni$  channels. A Mulliken charge analysis of **3** shows that of the two recipient carbon centres, the more substituted is more electrophilic [+0.336 *vs.* +0.158 at the RHF/6-31+G(d) level]. This could mean that the probability of **3** entering the channel to form **4** is higher than that for the competing formation of **5**.

The *ab initio* calculations predict (i) that the relative proportions of products **4** and **5** (from **3**) should be comparable if the rates of the two reactions are controlled by the relative barriers to the transition states, (ii) should frequency factors control the kinetically controlled reactions, **4** will be the major product, and (iii) if the reaction of **3** to **4** is reversible under the reaction conditions, thermodynamic product **5** may be formed in the higher yield.

## 2. The reactions of **3**, **4** and **5** in the condensed phase

The computed results shown in Fig. 1 apply to reactions carried out in the absence of solvent. Does such a scenario also pertain

**Table 1** Energies of stable ions and transition states shown in Fig. 1 together with geometries of transition states at the MP2-Fc/6-31+G(d) level<sup>a</sup>

Species	Energy/hartrees (kJ mol <sup>-1</sup> )	Geometry			
		Bond lengths/Å		Bond angles/°	
<b>3</b>	-305.996 752 1 (0)	See Supplementary data			
<b>4</b>	-305.997 086 (-1)				
<b>5</b>	-306.028 400 4 (-83)				
<b>C</b>	-305.970 138 3 (+70)	$C^1C^2$	1.452	$C^1C^2C^3$	122.45
		$C^2C^3$	1.509	$C^2C^3C^4$	95.09
		$C^3C^4$	1.525	$C^3C^4O^5$	99.49
		$C^4O^5$	1.404	$O^5C^2O^6$	163.45
		$C^1O^6$	1.410	$C^2C^1O^6$	80.77
		$C^2O^6$	1.850	$O^5C^2C^1O^6$	172.52
		$C^2O^5$	2.005		
<b>D</b>	-305.964 541 5 (+69)	$C^1C^2$	1.437	$C^1C^2C^3$	108.54
		$C^2C^3$	1.509	$C^2C^3C^4$	102.40
		$C^3C^4$	1.562	$C^3C^4O^5$	111.50
		$C^4O^5$	1.390	$O^5C^1O^6$	140.35
		$C^1O^5$	2.090	$C^1C^2O^6$	79.81
		$C^1O^6$	1.840	$C^3C^2O^6$	125.00
		$C^2O^6$	1.426	$O^5C^1C^2O^6$	-163.13

<sup>a</sup> Full details of bond lengths and angles are available as supplementary material (SUPPL. NO. 57382, 5 pp.). For details of the Supplementary Publications Scheme see 'Instructions for Authors', *J. Chem. Soc., Perkin Trans. 2*, available via the RSC Web page (<http://www.rsc.org/authors>).

**Table 2** Base catalysed solution reactions of **3**, **4** and **5**<sup>a</sup>

Reactant	System <sup>b</sup>	Time/h	Ratio ( <b>3</b> : <b>4</b> : <b>5</b> ) <sup>c</sup>
<b>3</b>	A	0.17	100:0:0
	A	1	77:3:20
	A	15	22:11:67
	A	30	20:10:70
	A	60	20:10:70
	B	0.17	73:2:25
	B	1	21:7:62
	B	15	11:11:78
	B	30	10:11:79
	B	60	9:13:78
<b>4</b>	A	3	0:100:0
	A	15	19:100:0
	A	30	27:100:9
	B	3	0:100:0
<b>5</b>	B	15	50:100:0
	B	30	24:100:20
	A	30	0:0:100
	B	30	0:0:100

<sup>a</sup> For experimental conditions see Experimental section. <sup>b</sup> System A: 10% NaOH, 100 °C. System B: NaH–tetrahydrofuran, 65 °C. <sup>c</sup> The ratio is obtained by comparing the areas under each peak (this ratio correlates closely with the ratios obtained using ion counts/peak). The error in each number within a ratio is *ca.* ± 5%.

to the analogous base catalysed reaction in solution? The reactions of **3**, **4** and **5** have been examined in two solvent systems, (a) 10% aqueous sodium hydroxide at 100 °C, and (b) sodium hydride–tetrahydrofuran at 65 °C. These systems were chosen because they were used previously in investigations of the Payne rearrangement (*cf.* ref. 1). Products were monitored at different reaction times using gas chromatography–mass spectrometry. The following observations can be made from the data recorded in Table 2: (i) the anion **3** converts to both **4** and **5**, with **5** being the major product, (ii) the four-membered ring system **4** converts slowly to the 3,4-epoxybutoxide anion **3**, which in turn forms **4** and **5**, (iii) the five-membered ring system **5** is stable under the reaction conditions, (iv) conversions of **3** to **4** and **5** are more facile than conversion of **4** to **3**, and (v) the  $S_Ni$  reac-

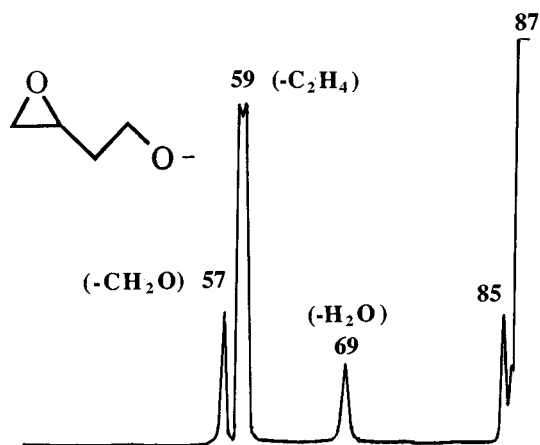


**Fig. 2** Collision induced  $\text{HO}^-$  negative ion chemical ionisation (MS-MS) mass spectrum of the 3,4-epoxybutoxide anion. VG ZAB 2HF mass spectrometer. For experimental conditions see Experimental section. Peak widths at half height:  $m/z$  69 ( $75.2 \pm 1.0$  V),  $m/z$  59 ( $95.8 \pm 1.0$  V).

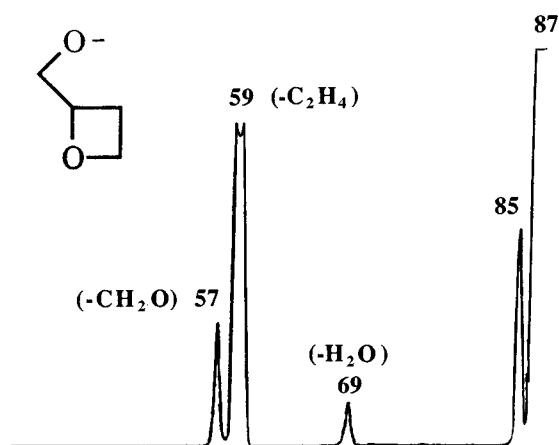


**Fig. 3** Collision induced mass spectrum of the  $(M-H)^-$  ion of 2-(oxiran-2-yl)ethan-1-ol. VG ZAB 2HF mass spectrometer. Peak widths at half height:  $m/z$  69 ( $72.0 \pm 1.0$  V),  $m/z$  59 ( $93.1 \pm 1.0$  V).

tions of **3** and **4** proceed more readily in the NaH-tetrahydrofuran system.

Thus reaction **3**→**5** is more favourable in solution than **3**→**4**. This is in contrast to the scenario predicted in Fig. 1 for a gas phase reaction. The slow conversion of **4**→**3** is not reflected in the ratio of products of **4** and **5** (from **3**) with increasing time because **4** constitutes only some 10% of the product mixture **4** and **5**. The  $\text{S}_{\text{Ni}}$  reactions of **3** proceed through transition states in which the charge is dispersed (relative to the reactant), so the reaction rates should not be significantly influenced by the relative permittivity of the solvent (78.5 for  $\text{H}_2\text{O}$ , 7.4 for tetrahydrofuran). Nor should the counter ion influence the relative reaction rates since it is  $\text{Na}^+$  in both systems. In contrast, the rates should be influenced by the solvating power of the solvent, *i.e.* a protic solvent like water will strongly solvate the anion centre and consequently retard an  $\text{S}_{\text{Ni}}$  reaction (compared with the same reaction performed in a non-protic solvent like tetrahydrofuran), as observed for the  $\text{S}_{\text{Ni}}$  reactions of **3**.

### 3. Gas phase cyclisations of the 3,4-epoxypropoxide anion

The collision induced mass spectra of the isomers **3**, **4** and **5** are shown in Figs. 2–4 (peak widths at half height of some fragment ions are recorded in the legends to Figs. 2–4). In our study of the Payne rearrangement, we used the loss of  $\text{CH}_2\text{O}$  from the  $(M-H)^-$  ion as a probe to test for the operation of the competing  $\text{S}_{\text{Ni}}$  reactions shown in Scheme 1.<sup>1</sup> In the present investigation, consideration of the spectra shown in Figs. 2–4 suggests

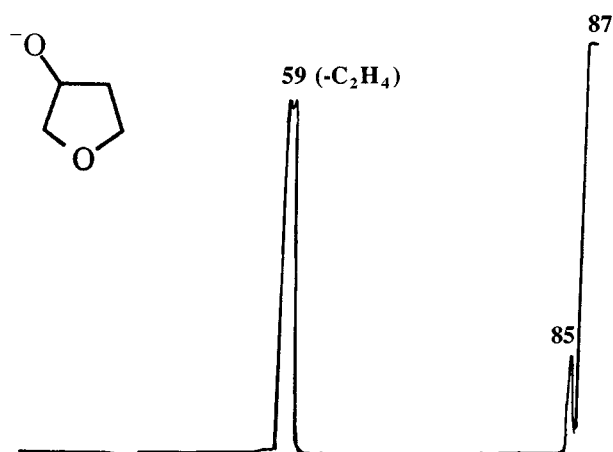
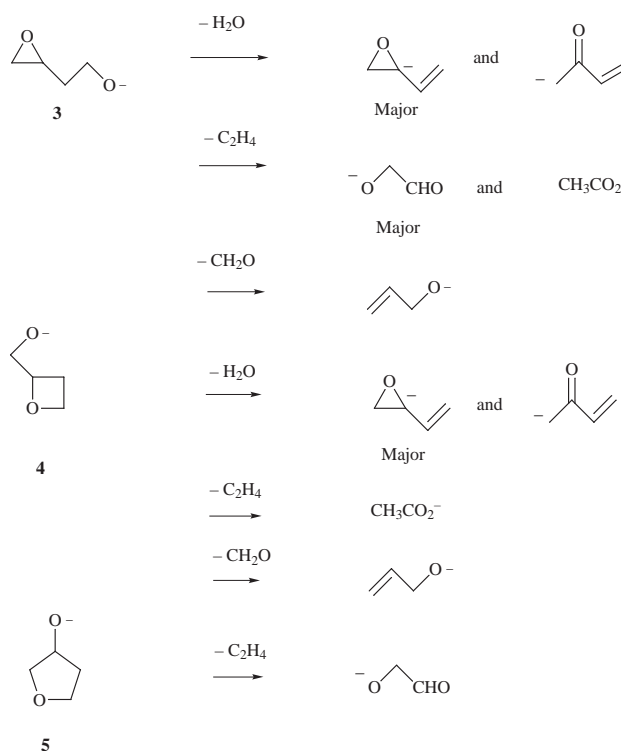


**Fig. 4** Collision induced mass spectrum of the  $(M-H)^-$  ion of tetrahydrofuran-3-ol. VG ZAB 2HF mass spectrometer. Peak width at half height:  $m/z$  59 ( $100.0 \pm 1.0$  V).


that three processes might provide information concerning the operation of the two  $\text{S}_{\text{Ni}}$  processes depicted in Fig. 1, *viz.*, the competitive losses of  $\text{H}_2\text{O}$ ,  $\text{C}_2\text{H}_4$  and  $\text{CH}_2\text{O}$  from  $(M-H)^-$  ions. We need to know the structures of each of these ions, together with their mechanisms of formation from **3**–**5** (as appropriate). The structures of the daughter ions formed from these processes have been determined by a comparison of the spectra [both collision induced and charge reversal (positive ion)<sup>4</sup> spectra] with those of authentic anions formed by independent syntheses. The product ion spectra are recorded in Table 3: the conclusions arising from these data are summarised in Scheme 3.



**Scheme 3**

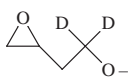
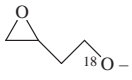
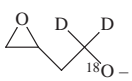
The spectra of deuterium and  $^{18}\text{O}$  labelled analogues of the 3,4-epoxybutoxide anion are listed in Table 4. The peak shapes of the broad peaks in the spectra of two labelled compounds are shown in Fig. 5: the example of a Gaussian peak (loss of  $\text{CH}_2\text{O}$ ) superimposed on the dish-shaped peak (loss of  $\text{C}_2\text{H}_2\text{D}_2$ ) (see Fig. 5A) is noteworthy. These spectra show that the losses of  $\text{H}_2\text{O}$  and  $\text{CH}_2\text{O}$  from the 3,4-epoxybutoxide anion

**Table 3** Spectra of product anions from **3–5** and known anions

Precursor ion	Product ion <i>m/z</i> (loss)	Mode	Spectrum [CA: <i>m/z</i> (loss) abundance] <sup>a</sup> [CR: <i>m/z</i> (abundance)]
<b>3</b>	69 (–H <sub>2</sub> O)	CR	69(1), 68(73), 66(4), 55(11), 54(5), 53(8), 52(6), 51(8), 50(15), 42(43), 41(27), 40(8), 39(100), 38(20), 37(13), 29(15), 27(25), 26(41), 25(8)
<b>4</b>	69 (–H <sub>2</sub> O)	CR	69(1), 68(59), 66(3), 55(10), 54(16), 53(17), 52(11), 51(16), 50(19), 42(22), 41(21), 40(12), 39(100), 38(22), 37(13), 29(22), 27(23), 26(33), 25(8)
		CR	69(1), 68(100), 66(6), 54(16), 53(12), 52(8), 51(12), 50(18), 42(6), 41(27), 40(10), 39(71), 38(21), 37(9), 29(18), 27(8), 26(10), 25(12)
<sup>–</sup> [CH <sub>2</sub> COCH=CH <sub>2</sub> ] <sup>b</sup> ( <i>m/z</i> 69)		CR	68(2), 66(1), 55(33), 54(8), 53(12), 52(7), 51(9), 50(19), 42(100), 41(33), 39(38), 37(10), 29(5), 27(46), 26(28), 25(10), 14(1)
<b>3</b>	59 (–C <sub>2</sub> H <sub>4</sub> )	CA CR	58(H <sup>+</sup> )100, 57(H <sub>2</sub> )65, 44(CH <sub>3</sub> )8, 31(CO)32, 29(CH <sub>2</sub> O)11 59(12), 58(29), 56(31), 45(11), 44(22), 43(15), 42(22), 41(20), 31(18), 30(22), 29(100), 28(29), 15(2)
<b>4</b>	59 (–C <sub>2</sub> H <sub>4</sub> )	CR	56(5), 45(42), 44(100), 43(34), 42(39), 41(19), 29(34), 28(28), 15(6), 14(4), 13(2), 12(1)
<b>5</b>	59 (–C <sub>2</sub> H <sub>4</sub> )	CR	59(14), 58(46), 56(42), 42(14), 41(10), 31(12), 30(32), 29(100), 28(29)
<sup>–</sup> OCH <sub>2</sub> CHO <sup>c</sup> ( <i>m/z</i> 59)		CA CR	58(H <sup>+</sup> )100, 57(H <sub>2</sub> )60, 31(CO)30, 29(CH <sub>2</sub> O)13 59(8), 58(33), 56(19), 42(24), 41(27), 31(31), 30(44), 29(100), 28(39)
CH <sub>3</sub> CO <sub>2</sub> <sup>–d</sup> ( <i>m/z</i> 59)		CR	56(4), 45(28), 44(100), 43(36), 42(38), 41(18), 29(12), 28(13), 15(10), 14(5), 13(2), 12(1)
<b>3</b>	57 (CH <sub>2</sub> O)	CA CR	56(H <sup>+</sup> )68, 55(H <sub>2</sub> )100, 41(CH <sub>4</sub> )28, 29(C <sub>2</sub> H <sub>4</sub> )36, 27(CH <sub>2</sub> O)58 56(12), 55(58), 53(14), 42(18), 41(20), 39(62), 38(18), 37(16), 29(100), 28(19), 27(68), 26(48), 25(15)
<b>4</b>	57 (CH <sub>2</sub> O)	CA	56(H <sup>+</sup> )65, 55(H <sub>2</sub> )100, 41(CH <sub>4</sub> )26, 29(C <sub>2</sub> H <sub>4</sub> )33, 27(CH <sub>2</sub> O)52
CH <sub>2</sub> =CHCH <sub>2</sub> O <sup>–e</sup> ( <i>m/z</i> 57)		CA CR	56(H <sup>+</sup> )65, 55(H <sub>2</sub> )100, 41(CH <sub>4</sub> )25, 29(C <sub>2</sub> H <sub>4</sub> )32, 27(CH <sub>2</sub> O)55 56(10), 55(64), 53(12), 42(12), 41(16), 39(54), 38(14), 37(12), 29(100), 28(26), 27(75), 26(50), 25(12)

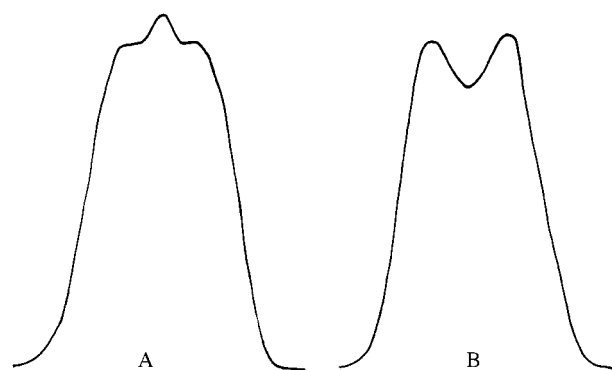
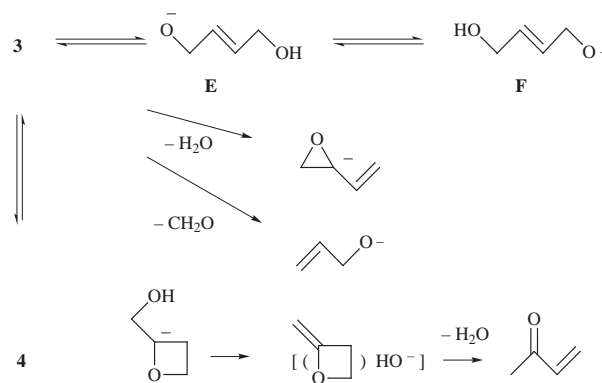
<sup>a</sup> The relative abundances of CR spectra are critically dependent upon the collision gas pressure. Discrepancies between the abundances of peaks in the charge reversal spectra of source formed product anions and in the spectra of authentic anions is to be expected. This is particularly apparent for the CR spectra of the [(M – H)<sup>–</sup> – C<sub>2</sub>H<sub>4</sub>]<sup>–</sup> ions and of CH<sub>3</sub>CO<sub>2</sub><sup>–</sup> and <sup>–</sup>CH<sub>2</sub>CHO. Even so, the spectra are quite characteristic, and there can be no doubt as to the structures of the two [(M – H)<sup>–</sup> – C<sub>2</sub>H<sub>4</sub>]<sup>–</sup> species. <sup>b</sup> Formed by deprotonation of methyl vinyl ketone. <sup>c</sup> Formed by reaction of HO<sup>–</sup> with 2,5-dihydroxy-1,4-dioxane. <sup>d</sup> Formed by deprotonation of acetic acid. <sup>e</sup> Formed by deprotonation of allyl alcohol.

**Table 4** Mass spectra of labelled 3,4-epoxybutoxide anions

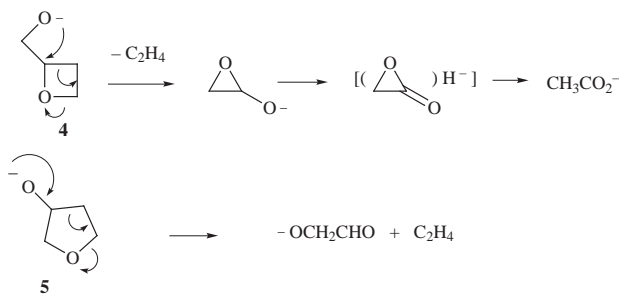
Anion	<i>m/z</i> (loss) abundance
	88(H <sup>+</sup> )55, 87(H <sub>2</sub> , D <sup>+</sup> )100, 71(H <sub>2</sub> O)20, 59(C <sub>2</sub> H <sub>2</sub> D <sub>2</sub> , CH <sub>2</sub> O)85, 57(CD <sub>2</sub> O)17
( <i>m/z</i> 89)	
	88(H <sup>+</sup> )45, 87(H <sub>2</sub> )92, 71(H <sub>2</sub> O)7, 69(H <sub>2</sub> <sup>18</sup> O)17, 61(C <sub>2</sub> H <sub>4</sub> )100, 59(CH <sub>2</sub> O)8, 57(CH <sub>2</sub> <sup>18</sup> O)16
( <i>m/z</i> 89)	
	90(H <sup>+</sup> )100, 89(H <sub>2</sub> , D <sup>+</sup> )82, 88(HD)18, 71(H <sub>2</sub> O)3, 69(H <sub>2</sub> <sup>18</sup> O)14, 61(CH <sub>2</sub> O, C <sub>2</sub> H <sub>2</sub> D <sub>2</sub> )85, 57(CD <sub>2</sub> <sup>18</sup> O)15
( <i>m/z</i> 91)	

principally involve the side chain oxygen of **3**, with the epoxide oxygen being involved to a lesser extent. We propose, from a consideration of the labelling and product ion data, that (i) anions **3** and **4** can interconvert under the reaction conditions, (ii) the loss of CH<sub>2</sub>O, and the major loss of H<sub>2</sub>O from **3** (and **4**) are fragmentations of **3**, but a minor proportion of these losses follow equilibration of the two oxygens by formation of **E** and **F** (see Scheme 4, **E** is formed by proton transfer within **3** from the 2 position to O<sup>–</sup>, followed by ring opening), and (iii) the methyl vinyl ketone enolate ion (the minor product resulting from loss of water) is formed exclusively from **4** (see Scheme 4).

The data considered so far suggest that **3** and **4** are interconvertible, but provide no evidence concerning the relationship between **4** and **5**. That information is forthcoming from a consideration of the various losses of ethene, processes which cannot occur directly from anion **3**. The product ion data summarised in Scheme 3 show that loss of C<sub>2</sub>H<sub>4</sub> from **4** yields

**Fig. 5** Peak profile of the broad peaks in the spectra of the (M – H)<sup>–</sup> ions of (A), 2-(oxiran-2-yl)ethan-1-[<sup>18</sup>O]ol, and (B) [1,1-<sup>2</sup>H<sub>2</sub>]-2-(oxiran-2-yl)ethan-1-ol**Scheme 4**

CH<sub>3</sub>CO<sub>2</sub><sup>–</sup> whereas the analogous loss from **5** forms <sup>–</sup>OCH<sub>2</sub>CHO. Suggested mechanisms for the formation of these ions are shown in Scheme 5. The formation of the acetate anion



from **4** is unusual, but is analogous to the mechanism proposed to account for the formation of  $(\text{MeCOCH}_2)^-$  from  $^-\text{CH}_2\text{CH}_2\text{-CHO}$ .<sup>5</sup> The process is slightly exothermic [ $\Delta H$  for the conversion of **4** to  $\text{CH}_3\text{CO}_2^-$  is calculated to be  $-23 \text{ kJ mol}^{-1(2)}$ : the high electron affinity of  $\text{CH}_3\text{CO}_2^-$  ( $297 \text{ kJ mol}^{-1(6)}$ ) is primarily responsible for the exothermicity of this process]. Both losses of ethene shown in Scheme 5 yield broad dish-shaped peaks (see Figs. 2–5). The corresponding peak in the spectrum (Fig. 2) of **3** corresponds to a mixture of  $\text{CH}_3\text{CO}_2^-$  and  $^-\text{OCH}_2\text{CHO}$  with the latter ion being the major contributor (see Scheme 3 and Table 3). It is also noteworthy that the width at half height of the composite peak for the loss of  $\text{C}_2\text{H}_4$  from **3** ( $95.8 \pm 1 \text{ V}$ ) is intermediate between those for the losses of  $\text{C}_2\text{H}_4$  from **4** ( $93.1 \pm 1 \text{ V}$ ) and **5** ( $100.0 \pm 1 \text{ V}$ ). Thus both **4** and **5** are formed from energised **3**, but since the spectra shown in Figs. 3 and 4 are different, ions **4** and **5** are not interconvertible under the reaction conditions.

## Conclusions

*Ab initio* calculations suggest that energised **3** should, in the absence of solvent, and under conditions of kinetic control, convert to the two  $\text{S}_{\text{N}}\text{i}$  products, **4** and **5**, in comparable yield if barriers to transition states alone determine the rates of the reactions. The relative barrier to the transition state for each of the competitive  $\text{S}_{\text{N}}\text{i}$  processes is primarily a function of (i) the angle of approach of  $\text{O}^-$  to the recipient carbon centre, and (ii) the difference in ring strain between reactant and transition state. If frequency factors control energy into the two reaction channels, then **4** should be the predominant product. If **3** and **4** are interconvertible under the reaction conditions, thermodynamic product **5** should be the major product.

Gas phase studies indicate that upon collisional activation (i) **3** undergoes competitive  $\text{S}_{\text{N}}\text{i}$  reactions to yield both **4** and **5** in comparable amounts, (ii) **4** is able to convert to **3**, and (iii) **5** does not convert to either **3** or **4**. These results are compatible with the theoretical predictions involving similar barrier heights, with frequency factors being of lesser importance in this system.

The condensed phase studies are different from those outlined above. The evidence suggests that in the solvent systems used, the kinetic product from **3** is **5**, rather than **4** (whereas in the gas phase **4** and **5** are formed to a similar degree).

## Experimental

### Mass spectrometric methods

Collisional activation (CA) mass spectra (MS–MS) were determined with a VG ZAB 2HF mass spectrometer.<sup>7</sup> Full operating details have been reported.<sup>8</sup> Specific details were as follows: the chemical ionisation slit was used in the chemical ionisation source, the ionising energy was 70 eV, the ion source temperature was 100 °C, and the accelerating voltage was 7 kV. The liquid samples were introduced through the septum inlet with no heating [measured pressure of sample  $1 \times 10^{-6}$  Torr (1 Torr = 133.322 Pa)]. Deprotonation was effected using  $\text{HO}^-$  (from  $\text{H}_2\text{O}$ : measured pressure  $1 \times 10^{-5}$  Torr). The estimated

source pressure was  $10^{-1}$  Torr. Argon was used in the second collision cell (measured pressure, outside the cell,  $2 \times 10^{-7}$  Torr), giving a 10% reduction in the main beam, equivalent to single collision conditions. Collision induced dissociation (CID) MS–MS measurements involved using the magnet to choose the ion under study [normally the  $(\text{M} - \text{H})^-$  species], collision activating it (see above), and scanning the electric sector to analyse the resultant product anions. Charge reversal (CR) (positive ion) MS–MS data for negative ions were obtained as for CA MS–MS data, except that the electric sector potential was reversed to allow the transmission of positively charged product ions (for full details see ref. 4). The recorded peak widths at half height are an average of five individual measurements.

### Ab initio calculations

The GAUSSIAN94<sup>3</sup> suite of programs was used for all calculations. The computational platforms used were a Silicon Graphics Indigo<sup>2</sup>xZ workstation and a Silicon Graphics Power Challenge. The geometries of the local minima and the transition states were optimised at the RHF/6-31+G(d) level of theory. Harmonic frequency analyses were performed on each stationary point in order to characterise them as either a local minimum or a transition state. A local minimum is characterised by possessing all real vibrational frequencies and its hessian matrix possessing all positive eigenvalues. A transition state is characterised by possessing one (and only one) imaginary frequency and its hessian matrix possessing one (and only one) negative eigenvalue. Intrinsic reaction coordinate (IRC) calculations were performed (beginning from both transition structures) to verify that each transition structure connected particular local minima. The energy of each structure at 0 K was calculated using MP2-Fc/6-31+G(d) level of theory. The energies include a scaled (0.8929) zero point vibrational energy correction based on the RHF/6-31+G(d) optimised geometry.

### Unlabelled compounds

Allyl alcohol, butadiene monoxide, crotonaldehyde, 2,5-dihydrofuran, 1,4-dioxane-2,3-diol and propylene oxide were commercial samples. Tetrahydrofuran-3-ol,<sup>9</sup> oxetan-2-ylmethanol<sup>10</sup> and 2-(oxiran-2-yl)ethan-1-ol<sup>11</sup> were prepared by reported procedures.

### Labelled compounds

Labelled compounds were synthesised as outlined below. The purity of all products was established by <sup>1</sup>H NMR and positive ion mass spectrometry. The extent of incorporation (of D and/or <sup>18</sup>O) was established by either positive or negative ion mass spectrometry.

**[1,1-<sup>2</sup>H<sub>2</sub>]-2-(Oxiran-2-yl)ethan-1-[<sup>18</sup>O]ol.** A mixture of vinylacetic acid (1 g), oxalyl chloride (1.22 g) and *N,N*-dimethylformamide (1 drop) in anhydrous diethyl ether (30 cm<sup>3</sup>) was stirred at 20 °C for 2 h under nitrogen. Distillation yielded but-3-enoyl chloride (0.8 g), which was added to a mixture of anhydrous tetrahydrofuran (10 cm<sup>3</sup>) and H<sub>2</sub><sup>18</sup>O (160 mg, 96% <sup>18</sup>O). The mixture was stirred at 20 °C for 12 h, the solvent removed *in vacuo*, the residue dissolved in diethyl ether (20 cm<sup>3</sup>), and added at 0 °C to a slurry of lithium aluminium deuteride (0.5 g) in diethyl ether (10 cm<sup>3</sup>). The mixture was heated at reflux for 3 h, cooled to 0 °C, water (5 cm<sup>3</sup>) was added followed by aqueous hydrogen chloride (saturated, 2 cm<sup>3</sup>). The organic layer was separated, the aqueous layer extracted with diethyl ether (2 × 30 cm<sup>3</sup>) and the combined organic extract dried (MgSO<sub>4</sub>), concentrated *in vacuo* and distilled to give [1,1-<sup>2</sup>H<sub>2</sub>]-but-3-en-1-[<sup>18</sup>O]ol (0.75 g, bp 109–111 °C at atmospheric pressure). *meta*-Chloroperbenzoic acid (3 g) was added, at 0 °C, to the labelled buten-1-ol (0.75 g) in dichloromethane (25 cm<sup>3</sup>), the mixture allowed to stir at 20 °C for 20 h, aqueous sodium hydroxide (10%, 12 cm<sup>3</sup>) was added, the organic layer separated and the aqueous layer extracted with dichloro-

methane ( $3 \times 20 \text{ cm}^3$ ). The combined organic extracts were dried ( $\text{MgSO}_4$ ), concentrated *in vacuo*, and the residue distilled to yield  $[1,1\text{-}^2\text{H}_2]\text{-2-(oxiran-2-yl)ethan-1-}[^{18}\text{O}]\text{ol}$  (0.45 g, overall yield 36%,  $^{18}\text{O} = 48\%$ ,  $^2\text{H}_2 = 99\%$ ).

**$[1,1\text{-}^2\text{H}_2]\text{-2-(Oxiran-2-yl)ethan-1-ol}$ .** The method is similar to that outlined above. Vinylacetic acid was reduced with lithium aluminium deuteride to yield  $[1,1\text{-}^2\text{H}_2]\text{-but-3-en-1-ol}$ , which was then epoxidised to yield  $[1,1\text{-}^2\text{H}_2]\text{-2-(oxiran-2-yl)ethan-1-ol}$  (overall yield 55%,  $^2\text{H}_2 = 99\%$ ).

**$2\text{-(Oxiran-2-yl)ethan-1-}[^{18}\text{O}]\text{ol}$ .** The method is similar to those outlined above except that  $\text{H}_2^{18}\text{O}$  and lithium aluminium hydride were used. Overall yield 46%,  $^{18}\text{O} = 48\%$ .

#### Condensed phase reactions

Products of the reactions outlined below were analysed using a Finnigan MAT GCQ mass spectrometer. Conditions: column phase RTX-SMS (length 30 cm, id 0.25 mm, GC fused silica capillary), He carrier gas. Initial column temperature, held at  $50^\circ\text{C}$  for 2 min, then the temperature increased at  $15^\circ\text{C}$  per minute. Retention times: **3** (4.05 min), **4** (3.23 min) and **5** (3.48 min).

**System A.** A mixture of  $2\text{-(oxiran-2-yl)ethan-1-ol}$  (0.5 g) in aqueous sodium hydroxide (10%,  $5 \text{ cm}^3$ ) was stirred under reflux for 15 h, cooled to  $20^\circ\text{C}$ , and aqueous hydrogen chloride (10%) was added dropwise until the pH was 6. The mixture was extracted with dichloromethane ( $4 \times 5 \text{ cm}^3$ ) and the combined organic extract was dried ( $\text{MgSO}_4$ ) and concentrated to give an oil (0.25 g). The reaction mixture was sampled at particular times, and the product composition analysed by GC-MS (see Table 2).

**System B.**  $2\text{-(Oxiran-2-yl)ethan-1-ol}$  (0.5 g) was added dropwise to a slurry of sodium hydride (1 mol equiv.) in tetrahydrofuran ( $10 \text{ cm}^3$ ) maintained at  $0^\circ\text{C}$ . The mixture was then heated at reflux for 15 h, cooled to  $0^\circ\text{C}$ , water ( $5 \text{ cm}^3$ ) was added, the mixture extracted with dichloromethane ( $4 \times 5 \text{ cm}^3$ ), the combined organic extracts dried ( $\text{MgSO}_4$ ), and concentrated to give an oil (0.4 g). The reaction mixture was sampled at particular times, and the product composition analysed by GC-MS.

Identical procedures were carried out with oxetan-2-ylmethanol and tetrahydrofuran-3-ol.

#### Acknowledgements

This project was financed by the Australian Research Council. J. M. H. and S. D. thank the ARC for a Ph.D. scholarship and a research associate position respectively.

#### References

- 1 S. Dua, M. S. Taylor, M. A. Buntine and J. H. Bowie, *J. Chem. Soc., Perkin Trans. 2*, 1997, 1991.
- 2 Data from: S. W. Benson, *Thermochemical Kinetics*, Wiley, New York, 1967.
- 3 GAUSSIAN94, Revision C3, M. J. Frisch, G. W. Trucks, H. B. Schlegel, P. M. W. Gill, B. G. Johnson, M. A. Robb, J. R. Cheeseman, T. Keith, G. A. Petersson, J. A. Montgomery, K. Raghavachari, M. A. Al-Latham, V. G. Zakrzewski, J. V. Ortiz, J. B. Foresman, J. Cioslowski, B. B. Stefanov, A. Nanayakkara, M. Challacombe, C. Y. Peng, P. V. Ayala, W. Chen, M. W. Wong, J. L. Andres, E. S. Replogle, R. Gomperts, R. L. Martin, D. J. Fox, J. S. Binkley, D. J. Defrees, J. Baker, J. P. Stewart, M. Head-Gordon, C. Gonzalez and J. A. Pople, Gaussian Inc., Pittsburgh, PA, 1995.
- 4 J. H. Bowie and T. Blumenthal, *J. Am. Chem. Soc.*, 1975, **97**, 2959; I. Howe, J. H. Bowie, J. E. Szulejko and J. H. Beynon, *Int. J. Mass Spectrom. Ion Phys.*, 1980, **34**, 99.
- 5 R. J. Waugh, R. N. Hayes, P. C. H. Eichinger, K. M. Downard and J. H. Bowie, *J. Am. Chem. Soc.*, 1990, **112**, 2537.
- 6 J. B. Cumming and P. Kebarle, *Can. J. Chem.*, 1978, **56**, 1.
- 7 VG ZAB 2HF, VG Analytical, Manchester, UK.
- 8 M. B. Stringer, J. L. Holmes and J. H. Bowie, *J. Am. Chem. Soc.*, 1986, **108**, 3888.
- 9 H. Wynberg and A. Bantjes, *Org. Synth.*, 1963, **Coll. Vol. 4**, 534.
- 10 A. O. Fitton, J. Hill, D. E. Jane and R. Millar, *Synthesis*, 1987, **12**, 1140.
- 11 H. C. Brown and G. J. Lynch, *J. Org. Chem.*, 1981, **46**, 930.

Paper 8/01172I

Received 10th February 1998

Accepted 21st April 1998